

## Isotopic ratio of radioactive iodine ( $^{129}\text{I}/^{131}\text{I}$ ) released from Fukushima Daiichi NPP accident

YASUTO MIYAKE,<sup>1\*</sup> HIROYUKI MATSUZAKI,<sup>1</sup> TAKESHI FUJIWARA,<sup>2</sup> TAKUMI SAITO,<sup>2</sup> TAKEYASU YAMAGATA,<sup>1,3</sup> MAKI HONDA<sup>3</sup> and YASUYUKI MURAMATSU<sup>4</sup>

<sup>1</sup>Department of Nuclear Engineering and Management, School of Engineering, The University of Tokyo, 7-3-1 Hongo, Bunkyo-ku, Tokyo 113-8656, Japan

<sup>2</sup>Nuclear Professional School, School of Engineering, The University of Tokyo, 2-22 Shirakatashirane, Tokai-mura, Naka-gun, Ibaraki 319-1188, Japan

<sup>3</sup>College of Humanities and Sciences, Nihon University, 3-25-40 Sakurajosui, Setagaya-ku, Tokyo 156-8550, Japan

<sup>4</sup>Department of Chemistry, Gakushuin University, Mejiro 1-5-1, Toshima-ku, Tokyo 171-8588, Japan

(Received March 2, 2012; Accepted May 28, 2012)

In March 2011, there was an accident at the Fukushima Daiichi Nuclear Power Plant (NPP) and a discharge of radionuclides resulting from a powerful earthquake. Considering the impact on human health, the radiation dosimetry is the most important for  $^{131}\text{I}$  among radionuclides in the initial stage immediately following the release of radionuclides. Since  $^{131}\text{I}$  cannot be detected after several months owing to its short half-life (8 days), the reconstruction by  $^{129}\text{I}$  (half-life:  $1.57 \times 10^7$  yrs) analysis is important. For this reconstruction, it is necessary to know the isotopic ratio of  $^{129}\text{I}/^{131}\text{I}$  of radioactive iodine released from the NPP. In this study, the  $^{129}\text{I}$  concentration was measured in several surface soil samples collected around the Fukushima Daiichi NPP for which the  $^{131}\text{I}$  level had already been determined. The surface deposition amount of  $^{129}\text{I}$  was between 15.6 and  $6.06 \times 10^3$  mBq/m<sup>2</sup> within the region 3.6 to 59.0 km distant from the NPP.  $^{129}\text{I}$  and  $^{131}\text{I}$  data had good linear correlation and the average isotopic ratio was estimated to be  $^{129}\text{I}/^{131}\text{I} = 31.6 \pm 8.9$  as of March 15, 2011.

Keywords: Fukushima, iodine, accelerator mass spectrometry, isotopic ratio, soil

### INTRODUCTION

On March 11, 2011, a powerful earthquake (magnitude 9.0) hit off the east coast of Japan. A tsunami triggered by the earthquake surged over the east coast of the Tohoku region, including Fukushima. The Fukushima Daiichi Nuclear Power Plant (NPP) lost its cooling ability and its reactors were heavily damaged. Owing to controlled venting and an unexpected hydrogen explosion, a large amount of radioactive material was released into the environment. Consequently, many residents living around the NPP were exposed to radiation. To evaluate the personal dosimetry precisely, it is essential to know the spatial distribution for each radionuclide and its temporal variation.

Iodine-131 (half-life: 8 days) is one of the most harmful radionuclides because it has the highest activity among radionuclides immediately after an accident and it causes thyroid cancer in children.

In the 1990s, many studies reported an increase in thyroid cancer in children due to the release of  $^{131}\text{I}$  during the Chernobyl accident in 1986 (Prisyazhniuk *et al.*, 1991; Kazakov *et al.*, 1992). The activity of  $^{131}\text{I}$  around an accident site needs to be known to evaluate precisely the health impact. However,  $^{131}\text{I}$  can hardly be detected after several years owing to its short half-life. The measurement of the activity of  $^{137}\text{Cs}$  (half-life: 30.1 y) is not completely suitable for the estimation of the  $^{131}\text{I}$  level because the two isotopes behave differently in the environment due to different chemical property (Hou *et al.*, 2003). On the other hand,  $^{129}\text{I}$  (half-life:  $1.57 \times 10^7$  yrs) is the optimum proxy for  $^{131}\text{I}$  because the two isotopes are of the same element and move identically after release during an accident. Moreover,  $^{129}\text{I}$  hardly decays and is considered to remain much longer in the environment than other proxies. Although the detection of  $^{129}\text{I}$  was complex and time-consuming when employing the radiochemical neutron activation analysis (RNAA) method, it became much easier to detect and with higher reliability following the development of the  $^{129}\text{I}$  detection system employing accelerator mass spectrometry (AMS). Several attempts were made to reconstruct the  $^{131}\text{I}$  level from the measure-

\*Corresponding author (e-mail: taizanhokuto62@gmail.com)

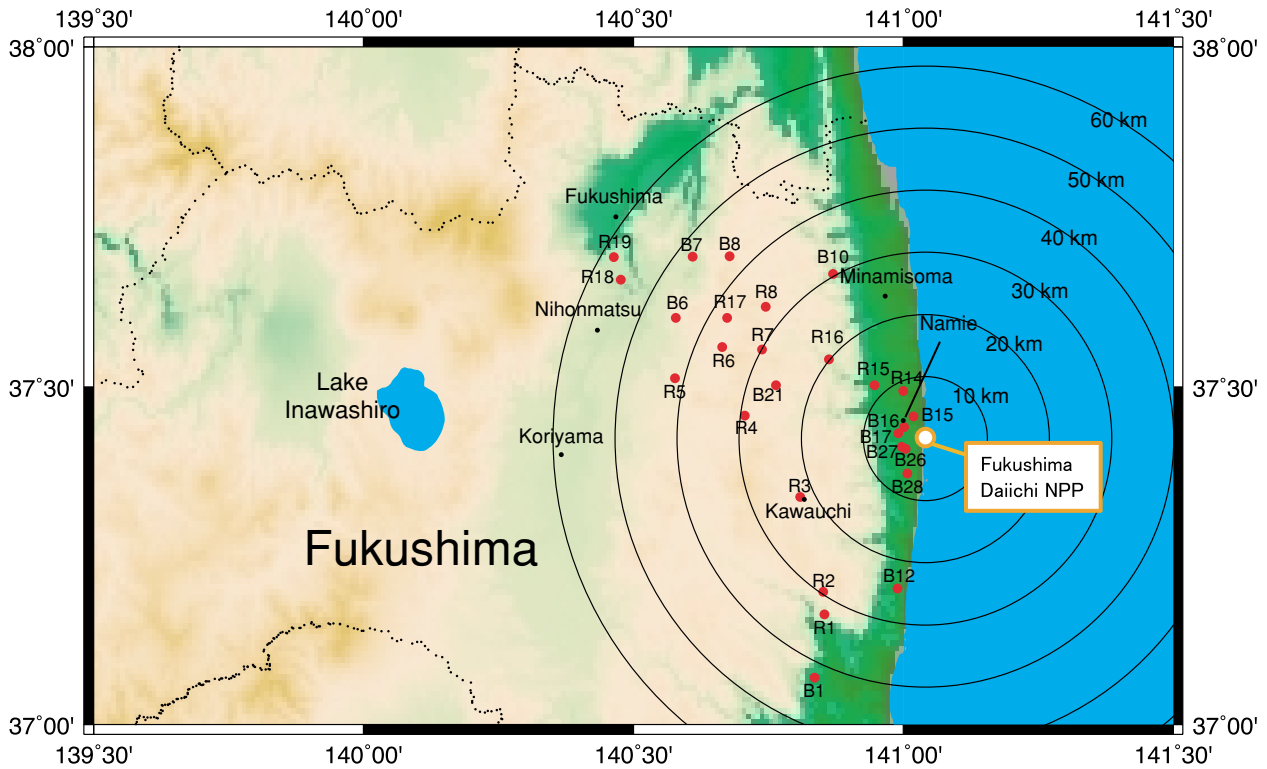


Fig. 1. Sampling locations in this study.

ment of  $^{129}\text{I}$ , but there were two problems in the Chernobyl case. First, the direct determination of the  $^{129}\text{I}/^{131}\text{I}$  ratio (decay-corrected for the release time) was not possible because of a lack of  $^{131}\text{I}$  data. The only way to estimate the ratio was a theoretical calculation, but calculation results were scattered from 11 to 34 (Michel *et al.*, 2005). Second, data for the background level of  $^{129}\text{I}$ , which already existed before the accident owing to atmospheric testing of nuclear bombs and releases from nuclear fuel reprocessing plants, were not available.

In the case of the Fukushima Daiichi NPP accident, several research teams approached the accident site and collected soil samples within two months (corresponding to 7–8 half-lives of  $^{131}\text{I}$ ) of the accident. The activities of collected soils, including the activity of  $^{131}\text{I}$  in the soils, were instantly measured by gamma-ray spectrometry. If  $^{129}\text{I}$  is measured in the same sample, the  $^{129}\text{I}/^{131}\text{I}$  ratio can be directly determined.

A detailed distribution of radioactivity (i.e., radioactivity map) is important in evaluating the health effects of radioactivity. In particular, details of the  $^{131}\text{I}$  distribution are indispensable. In the near future, extensive  $^{129}\text{I}$  analysis should serve for  $^{131}\text{I}$  reconstruction; for this purpose, a precise  $^{129}\text{I}/^{131}\text{I}$  ratio will be required.

In this study, the  $^{129}\text{I}$  concentration was measured for selected soil samples for which  $^{131}\text{I}$  had already been de-

termined by gamma-ray spectrometry in April 2011. From the datasets, we estimated the  $^{129}\text{I}/^{131}\text{I}$  ratio at the time of the release and we discuss the dispersion of the results.

## METHODS

Fujiwara *et al.* (2012) collected 50 surface soil samples around the Fukushima Daiichi NPP on April 20, 2011. Soil samples collected with a soil sampler (5 cm in diameter and 5 cm in height) were put into a U8 standard vessel after being roughly homogenized and dried. The results of the gamma-ray spectrometry for the samples, including results for  $^{131}\text{I}$  as well as  $^{134}\text{Cs}$  and  $^{137}\text{Cs}$ , were reported elsewhere (Fujiwara *et al.*, 2012). Twenty-seven of the 50 samples were selected in this study to measure the  $^{129}\text{I}$  concentration. Figure 1 shows the 27 sampling locations, which were mainly in forests and rice fields. Soil samples were homogenized again more completely and 0.1–0.2 g was then taken for  $^{129}\text{I}$  measurement. The complete homogenization is indispensable for the selected 0.1–0.2 g to be representative of the bulk. The following procedures are based on the work of Muramatsu *et al.* (2008). Each soil sample was combusted in a quartz tube with vanadium pentoxide, and outgas was trapped in alkali solution containing 2% tetramethyl ammonium hydroxide (TMAH) and 0.1%  $\text{Na}_2\text{SO}_3$ . An aliquot was taken

Table 1. Summary of analytical results

Sample ID	Field type <sup>(1)</sup>	Dry soil weight (g)	<sup>131</sup> I <sup>(2)</sup> (10 <sup>8</sup> atoms/g)	Analyzed soil weight (g)	Carrier ( <sup>127</sup> I) (mg)	AMS results <sup>(3)</sup> (×10 <sup>-12</sup> )	<sup>127</sup> I (ppm)	<sup>129</sup> I (10 <sup>9</sup> atoms/g)	<sup>129</sup> I (mBq/m <sup>2</sup> )	<sup>129</sup> I/ <sup>127</sup> I (×10 <sup>-8</sup> )	<sup>129</sup> I/ <sup>131</sup> I	Distance from Fukushima Daiichi NPP (km)
R1	Forest	135.6	0.118 ± 0.005	0.1361	1.00	7.5 ± 0.13	11.4 ± 0.1	0.28 ± 0.01	27.2 ± 0.5	0.52 ± 0.01	23.8 ± 1.0	33.4
R2	Forest	120.9	0.040 ± 0.003	0.1227	1.00	5.0 ± 0.10	11.4 ± 0.1	0.21 ± 0.00	17.8 ± 0.3	0.38 ± 0.01	51.4 ± 3.9	30.3
R3	Urban areas	132.1	0.122 ± 0.005	0.1506	1.00	12.3 ± 0.20	2.8 ± 0.0	0.42 ± 0.01	39.9 ± 0.7	3.21 ± 0.06	34.7 ± 1.5	22.7
R4	Forest	145.0	0.126 ± 0.005	0.1649	1.00	4.9 ± 0.09	2.1 ± 0.0	0.15 ± 0.00	15.6 ± 0.3	1.54 ± 0.03	12.0 ± 0.5	30.0
R5	Forest	152.8	0.127 ± 0.005	0.1673	1.00	15.4 ± 0.24	1.5 ± 0.0	0.48 ± 0.01	51.9 ± 0.8	6.48 ± 0.11	37.6 ± 1.6	42.2
R6	Forest	105.4	0.247 ± 0.008	0.1319	1.00	10.5 ± 0.17	9.3 ± 0.0	0.82 ± 0.01	61.3 ± 1.1	1.85 ± 0.03	33.1 ± 1.2	36.4
R7	Forest	128.9	0.731 ± 0.012	0.1068	2.00	25.6 ± 0.52	11.2 ± 0.1	2.48 ± 0.05	227.9 ± 4.6	4.66 ± 0.10	33.9 ± 0.9	30.5
R8	Forest	135.7	1.991 ± 0.020	0.1167	5.00	32.7 ± 0.66	8.0 ± 0.0	7.28 ± 0.15	703.9 ± 14.2	19.05 ± 0.39	36.5 ± 0.8	33.9
R14	Urban areas	146.9	0.245 ± 0.006	0.1280	1.00	12.4 ± 0.25	4.6 ± 0.0	0.50 ± 0.01	52.1 ± 1.0	2.26 ± 0.05	20.3 ± 0.7	8.6
R15	Vegetable field	140.3	1.574 ± 0.018	0.1230	10.00	10.0 ± 0.15	9.5 ± 0.1	4.17 ± 0.06	417.2 ± 6.2	9.27 ± 0.15	26.5 ± 0.5	12.1
R16	Vegetable field	133.6	5.345 ± 0.035	0.1563	25.00	32.1 ± 0.38	7.0 ± 0.1	26.59 ± 0.32	2533.2 ± 30.3	79.92 ± 1.21	49.8 ± 0.7	20.4
R17	Forest	131.8	0.560 ± 0.011	0.1227	5.00	7.9 ± 0.12	11.4 ± 0.0	1.64 ± 0.02	154.3 ± 2.3	3.06 ± 0.05	29.3 ± 0.7	37.9
R18	Urban areas	147.8	0.379 ± 0.008	0.1307	5.00	4.7 ± 0.10	5.8 ± 0.1	0.91 ± 0.02	95.5 ± 2.0	3.30 ± 0.08	23.9 ± 0.7	56.2
R19	Urban areas	111.3	0.032 ± 0.003	0.1282	1.00	5.3 ± 0.11	9.5 ± 0.0	0.21 ± 0.00	16.3 ± 0.3	0.40 ± 0.01	64.4 ± 5.8	59.0
B1	Rice field	114.8	0.206 ± 0.007	0.1216	1.00	14.7 ± 0.32	5.2 ± 0.1	0.64 ± 0.01	52.3 ± 1.1	2.61 ± 0.06	31.0 ± 1.2	43.4
B6	Rice field	132.6	0.262 ± 0.007	0.1331	2.00	10.3 ± 0.14	11.2 ± 0.1	0.79 ± 0.01	74.6 ± 1.0	1.49 ± 0.02	30.1 ± 0.9	45.3
B7	Rice field	140.2	0.264 ± 0.007	0.1348	1.00	20.5 ± 0.43	6.7 ± 0.0	0.78 ± 0.02	77.5 ± 1.6	2.44 ± 0.05	29.4 ± 1.0	48.3
B8	Rice field	108.4	1.581 ± 0.020	0.1198	10.00	6.8 ± 0.13	9.0 ± 0.1	2.90 ± 0.05	223.8 ± 4.2	6.85 ± 0.14	18.3 ± 0.4	43.8
B10	Rice field	132.6	0.462 ± 0.011	0.1430	5.00	6.1 ± 0.12	6.3 ± 0.1	1.08 ± 0.02	102.2 ± 2.0	3.61 ± 0.08	23.4 ± 0.7	30.9
B12	Rice field	128.9	2.257 ± 0.022	0.1329	20.00	16.5 ± 0.27	4.8 ± 0.0	12.86 ± 0.21	1181.6 ± 19.5	56.01 ± 0.93	57.0 ± 1.1	25.1
B15	Rice field	126.7	7.740 ± 0.041	0.1594	25.00	20.5 ± 0.33	12.2 ± 0.1	16.62 ± 0.27	1501.2 ± 24.5	28.61 ± 0.52	21.5 ± 0.4	4.1
B16	Rice field	128.7	1.911 ± 0.019	0.1413	20.00	10.1 ± 0.13	6.8 ± 0.0	7.36 ± 0.09	675.3 ± 8.4	23.00 ± 0.29	38.5 ± 0.6	3.9
B17	Rice field	124.8	17.124 ± 0.063	0.1250	25.00	54.3 ± 0.62	2.0 ± 0.0	56.37 ± 0.65	5015.8 ± 57.6	595.51 ± 6.95	32.9 ± 0.4	4.5
B21	Rice field	129.1	0.380 ± 0.009	0.1299	5.00	5.9 ± 0.12	10.2 ± 0.0	1.14 ± 0.02	105.1 ± 2.1	2.37 ± 0.05	30.0 ± 0.9	25.9
B26	Rice field	131.9	4.095 ± 0.031	0.1469	25.00	11.7 ± 0.22	1.2 ± 0.0	10.24 ± 0.19	963.0 ± 18.1	176.56 ± 3.63	25.0 ± 0.5	3.6
B27	Rice field	130.3	19.488 ± 0.065	0.1246	25.00	62.6 ± 0.71	1.9 ± 0.0	65.22 ± 0.74	6057.6 ± 68.5	719.94 ± 8.95	33.5 ± 0.4	4.1
B28	Rice field	133.5	3.578 ± 0.027	0.1550	25.00	13.2 ± 0.24	1.4 ± 0.0	10.92 ± 0.20	1039.6 ± 19.1	168.97 ± 3.33	30.5 ± 0.6	6.5

(1) Classification of field type was quoted by Fujiwara et al. (2012). Field type is forest, rice field, vegetable field, and others, mostly urban areas.

(2) <sup>131</sup>I data are decay-corrected as of March 15, 2011.

(3) AMS results were normalized to the standard Z94-0596 provided by PRIME Lab., Purdue University.

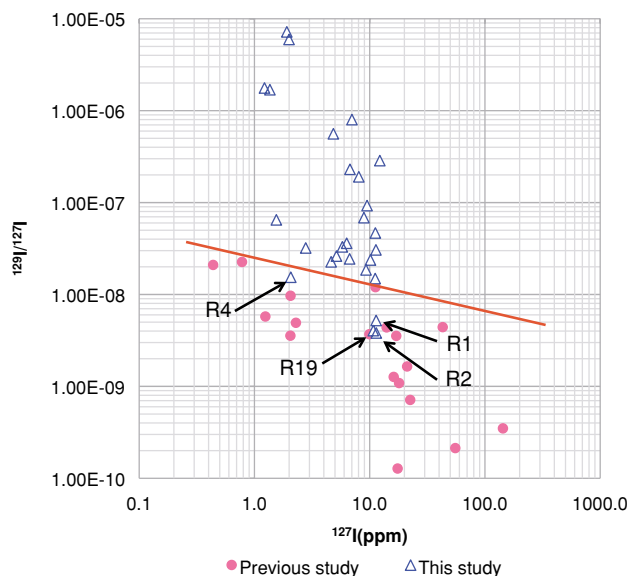


Fig. 2.  $^{129}\text{I}/^{127}\text{I}$  data obtained in this study plotted against the  $^{127}\text{I}$  concentration compared with data obtained in previous studies before the accident.

from the trap solution for the determination of the  $^{127}\text{I}$  (stable iodine) concentration by inductively coupled plasma mass spectrometry (ICP-MS). A proper quantity of the iodine carrier (with  $^{129}\text{I}/^{127}\text{I} = 1.7 \times 10^{-13}$ ) was added to the remainder of the trap solution, from which the iodine fraction was purified by solvent extraction and back extraction. For these manipulations, carbon tetrachloride was used as organic solvent. Under an acidic condition, 5%  $\text{NaNO}_2$  was added and iodide was then transformed to iodine and extracted into organic phase. Thereafter, iodine was back extracted into aqueous solution as  $\text{I}^-$  by adding 5%  $\text{Na}_2\text{SO}_3$ . Finally, silver iodide precipitation was obtained by adding silver nitrate solution. The precipitation was washed first with ammonia and then with pure water and dried well, and thereafter mixed with niobium powder and pressed into a cathode for the target at the ion source for AMS.  $^{129}\text{I}$ -AMS was performed at MALT (Micro Analysis Laboratory, Tandem Accelerator), The University of Tokyo (Matsuzaki *et al.*, 2007a). AMS results were normalized to the standard Z94-0956 provided by PRIME Lab, Purdue University (Sharma *et al.*, 1997).

## RESULTS AND DISCUSSION

### $^{129}\text{I}/^{131}\text{I}$ ratio

All analytical results are summarized in Table 1 together with  $^{131}\text{I}$  data. Analyzed samples included eight soils from forests, two soils from vegetable fields and 13 soils from rice fields (Fujiwara *et al.*, 2012). The  $^{127}\text{I}$  concentration ranged from 1.22 to 12.24 ppm. The surface

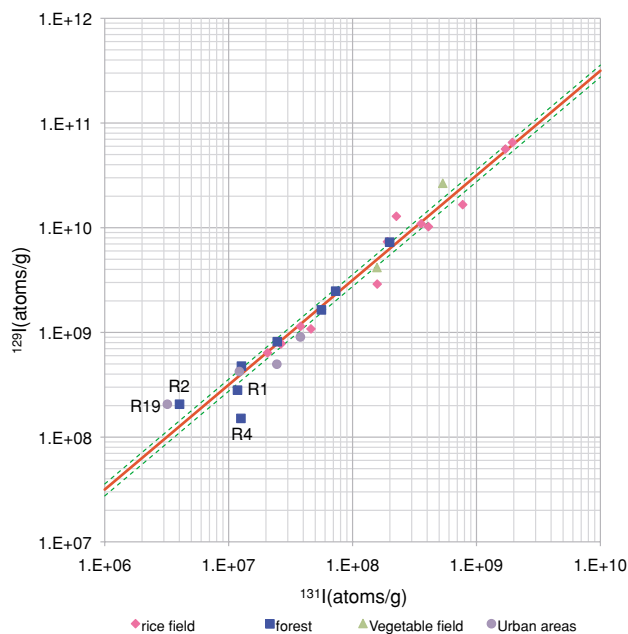


Fig. 3. Isotopic ratio ( $^{129}\text{I}/^{131}\text{I}$ ) of radioactive iodine. The solid line shows  $^{129}\text{I}/^{131}\text{I} = 31.6$  and the broken lines show the  $\pm 1$ -sigma range.

deposition amount of  $^{129}\text{I}$  ranged from  $15.6$  to  $6.06 \times 10^3$   $\text{mBq}/\text{m}^2$  in the region 3.6 to 59.0 km distant from the Fukushima Daiichi NPP.

Iodine-131 data were decay-corrected to March 15, 2011, when the highest rise in the air dose rate was recorded at monitoring posts of the Fukushima Daiichi NPP (TEPCO, 2011a), because we consider the day on which radionuclides were released into the environment as being important in the evaluation of the effect on human health.

It is important to note that  $^{129}\text{I}$  was already present before the Fukushima Daiichi NPP accident owing to atmospheric nuclear testing held in the 1950s and 1960s, and later, discharge from spent-nuclear-fuel reprocessing plants. Therefore, the  $^{129}\text{I}$  signal from the accident origin has to be distinguished from the background level before the accident. Figure 2 compares the  $^{129}\text{I}/^{127}\text{I}$  results obtained in this study and those obtained in previous works by analyzing soils collected from several locations in Japan before the accident (Matsuzaki *et al.*, 2007b; Muramatsu *et al.*, 2008). In Fig. 2,  $^{129}\text{I}/^{127}\text{I}$  data are plotted against the  $^{127}\text{I}$  concentration and moderate negative correlation is observed before the accident. This implies that the  $^{129}\text{I}/^{127}\text{I}$  ratio in the previous studies tends to depend on the  $^{127}\text{I}$  concentration in the soil. On the other hand, in this study, the  $^{129}\text{I}/^{127}\text{I}$  ratio is not reliant on the  $^{127}\text{I}$  concentration. Although we could not decisively determine the background level (since data for the region around the Fukushima Daiichi NPP before the accident

are not available any more), at least four data (R1, R2, R4 and R19) in this study are completely within the background region (below the line indicated in Fig. 2). Therefore, these four data were removed from the calculation of the mean isotopic ratio.

Eliminating these four data, we obtained the mean isotopic ratio  $^{129}\text{I}/^{131}\text{I} = 31.6 \pm 8.9$ . Figure 3 shows the relationship between the  $^{129}\text{I}$  concentration and  $^{131}\text{I}$  concentration.

The data variance is considerably larger than possible errors originating from analytical errors for AMS and ICP-MS, and uncertainty in the chemical yield in the iodine extraction procedure. Another possible reason for the data variance is that the radioactive iodine was released from multiple sources during the Fukushima Daiichi NPP accident. At least three different reactors at the Fukushima Daiichi NPP released radioactive material during the accident period. If the fuel-burn condition for each reactor differed, so may have the isotopic ratio  $^{129}\text{I}/^{131}\text{I}$ . However, we have not yet determined any clear correlation between the  $^{129}\text{I}/^{131}\text{I}$  ratio and the direction or distance from the NPP. More detailed analysis and data accumulation are required to examine this issue in the future.

Fujiwara *et al.* (2012) observed specific gamma rays from  $^{129\text{m}}\text{Te}$  in a few soil samples on April 20. If all detected  $^{129\text{m}}\text{Te}$  had decayed to  $^{129}\text{I}$  at the time of AMS measurement, then  $^{129\text{m}}\text{Te}$  should contribute at most 5% of the total amount of  $^{129}\text{I}$ , which is less than the scattering of the  $^{129}\text{I}/^{131}\text{I}$  ratio.

#### Estimation from fuel-burnt time

To see a consistency of our data to the theoretical calculation,  $^{129}\text{I}/^{131}\text{I}$  ratio in the nuclear reactor was roughly estimated as following. Note here is that this calculation includes large uncertainty and the aim of the calculation is just to check the consistency.

In the reactor, a fission product such as  $^{131}\text{I}$  is produced according to its fission yield as the  $^{235}\text{U}$  fuel is burnt.

Considering the origin of  $^{131}\text{I}$  is direct fission from  $^{235}\text{U}$ , the number of  $^{131}\text{I}$  atoms,  $N_{131}$  is as follows:

$$\frac{dN_{131}}{dt} = F \times \eta_{131} - \lambda_{131} \times N_{131}. \quad (1)$$

Here,  $F$  is the fission rate of  $^{235}\text{U}$ ,  $\eta_{131}$  is the fission yield of  $^{131}\text{I}$ ,  $\lambda_{131}$  is the decay constant of  $^{131}\text{I}$ , and  $t$  is the fuel-burnt time. As  $F$  is generally constant (with the initial condition  $N_{131} = 0$  at  $t = 0$ ),

$$N_{131} = \frac{F\eta_{131}}{\lambda_{131}} \left(1 - e^{-\lambda_{131}t}\right). \quad (2)$$

Similarly, in the case of  $^{129}\text{I}$ ,

$$N_{129} = \frac{F\eta_{129}}{\lambda_{129}} \left(1 - e^{-\lambda_{129}t}\right). \quad (3)$$

Considering that the fuel-burnt time is longer than the  $^{131}\text{I}$  half-life 8 days,

$$N_{131} = F \times \eta_{131} / \lambda_{131}. \quad (4)$$

On the other hand,  $\lambda_{129}t \ll 1$  holds; thus,

$$N_{129} = F \times \eta_{129} \times t. \quad (5)$$

Dividing Eq. (5) by Eq. (4), using  $\eta_{131} = 2.88\%$  and  $\eta_{129} = 0.71\%$  (Nichols *et al.*, 2008), the isotopic ratio is obtained as:

$$\frac{^{129}\text{I}}{^{131}\text{I}} = \frac{N_{129}}{N_{131}} = 0.021t. \quad (6)$$

According to Eq. (6),  $^{129}\text{I}/^{131}\text{I}$  is determined only by  $t$ .

Note that  $^{131}\text{I}$  can be produced by the decays of  $^{131}\text{Te}$  and  $^{131\text{m}}\text{Te}$  that are produced by the neutron capture of  $^{130}\text{Te}$ .  $^{129}\text{I}$  also has similar production path. As  $^{130}\text{Te}$  is almost stable, the number of  $^{130}\text{Te}$  in the reactor is written like Eq. (5):

$$N_{130} = F \times \eta_{130} \times t. \quad (7)$$

Here, again  $F$  is the fission rate of  $^{235}\text{U}$ ,  $\eta_{130}$  is the fission yield of  $^{130}\text{Te}$  and  $t$  is the fuel-burnt time. Knowing typical thermal neutron flux in the Boiling Water Reactor (BWR), like the Fukushima Daiichi NPP, is  $10^{12}$ – $10^{15}$ /s/cm<sup>2</sup>, and the neutron capture cross sections are 0.27 barn and 0.02 barn for  $^{130}\text{Te}(n, \gamma)^{131}\text{Te}$ ,  $^{130}\text{Te}(n, \gamma)^{131\text{m}}\text{Te}$ , respectively (Mughabghab and Garber, 1973). The production rates per a target nucleus ( $^{130}\text{Te}$ ) are at most  $2.7 \times 10^{-10}$ /s and  $0.2 \times 10^{-10}$ /s, respectively. Because the half-lives of  $^{131}\text{Te}$  and  $^{131\text{m}}\text{Te}$  are short (30 h and 25 m, respectively), the number of  $^{131}\text{I}$  produced by this path is of the order of  $F$  [s]  $\times \eta_{130} \times t$  [s]  $\times 3 \times 10^{-10}$ . The fuel-burnt time is no more than 10 y, i.e.,  $3 \times 10^8$  s, and  $\eta_{130}$  is 1.81% (Shibata *et al.*, 2011), the number of  $^{131}\text{I}$  via neutron capture is no more than  $F \times 0.00163$ . This is negligibly small compared with the direct fission production of  $F \times 2.8 \times 10^4$  (calculated from Eq. (4)). The situation for  $^{129}\text{I}$  is similar. Thus, it is enough to evaluate Eq. (6) for the estimation of  $^{129}\text{I}/^{131}\text{I}$  ratio.

Referring to the operation records of TEPCO (TEPCO 2004, 2005a, 2005b, 2005c, 2006, 2007, 2008a, 2008b, 2008c, 2009a, 2009b, 2010a, 2010b, 2011b, 2011c), a

nuclear reactor is stopped for regular inspection after every 300 to 400 days of operation. About one-fifth of used nuclear fuel assemblies are replaced with new assemblies during each regular inspection. From the history of operation times and the number of replaced fuel assemblies, the actual fuel-burn time at the time of the accident can be estimated. Although complete records were unavailable from Internet materials, the estimated fuel-burn time falls between 850 to 1000 days for Units 1, 2, and 3. This corresponds to  $^{129}\text{I}/^{131}\text{I} = 18$  to 21 as of March 11 according to Eq. (6). The result of this study ( $^{129}\text{I}/^{131}\text{I} = 31.6 \pm 8.9$  on March 15) corresponds to  $^{129}\text{I}/^{131}\text{I} = 22.3 \pm 6.3$  as of March 11, which is well consistent with the above calculation.

However, several parameters such as the fission rate  $F$  should have fluctuated depending on the reactor output. We do not know which part of the damaged fuel assembly actually contributed to the radioactive discharge. This cannot be observed until the insides of the reactors are unveiled. Additionally, mixed plutonium–uranium oxide fuel has partly been used and this effect should be taken into account. Therefore, the theoretical estimation should contain significant error, and measurements are thus indispensable.

## CONCLUSIONS

The  $^{129}\text{I}$  concentration was measured for selective surface soil samples collected around the Fukushima Daiichi NPP for which the  $^{131}\text{I}$  level had already been determined. The surface deposition amount of  $^{129}\text{I}$  was between 15.6 and  $6.06 \times 10^3$  mBq/m<sup>2</sup> in the region 3.6 to 59.0 km distant from the NPP.  $^{129}\text{I}$  and  $^{131}\text{I}$  data had good linear correlation. The mean isotopic ratio of  $^{129}\text{I}/^{131}\text{I}$  was  $31.6 \pm 8.9$  as of March 15, 2011. Such isotopic ratio data are important in reconstructing the  $^{131}\text{I}$  distribution from the detailed analysis of  $^{129}\text{I}$  in the future. The result of this study still includes approximately 30% error for the mean isotopic ratio, and more detailed analysis and data accumulation are required.

**Acknowledgments**—We wish to thank Mr. Nakano and Ms. Tsuchiya at School of Engineering, The University of Tokyo for experimental assistance.

## REFERENCES

- Fujiwara, T., Saito, T., Muroya, Y., Yamashita, Y., Nagasaki, S., Katsumura, Y., Tanaka, S. and Uesaka, M. (2012) Isotopic ratio and vertical distribution of radionuclides in soil affected by the accident of Fukushima Daiichi nuclear power plants. *J. Environ. Radioact.* (in press).
- Hou, X. L., Fogh, C. L., Kucera, J., Andersson, K. G., Dahlgard, H. and Noelsen, S. P. (2003) Iodine-129 and Caesium-137 in Chernobyl contaminated soil and their chemical fractionation. *Sci. Total Environ.* **308**, 97–109.
- Kazakov, V. S., Demidchik, E. P. and Astakhova, L. N. (1992) Thyroid cancer after Chernobyl. *Nature* **359**, 21.
- Matsuzaki, H., Nakano, C., Tsuchiya, S. Y., Kato, K., Maejima, Y., Miyairi, K., Wakasa, S. and Aze, T. (2007a) Multi-nuclide AMS performances at MALT. *Nuclear Instr. Methods Phys. Res.* **B259**, 36–40.
- Matsuzaki, H., Muramatsu, Y., Kato, K., Yasumoto, M. and Nakano, C. (2007b) Development of  $^{129}\text{I}$ -AMS system at MALT and measurements of  $^{129}\text{I}$  concentrations in several Japanese soils. *Nucl. Instr. Methods Phys. Res.* **B259**, 721–726.
- Michel, R., Handl, J., Ernst, T., Botsch, W., Szidat, S., Schmidt, A., Jakob, D., Beltz, D., Romantschuk, L. D., Synal, H.-A., Schnabel, C. and Lépez-Gutiérrez, J. M. (2005) Iodine-129 soils from Northern Ukraine and the retrospective dosimetry of the iodine-131 exposure after the Chernobyl accident. *Sci. Total Environ.* **340**, 35–55.
- Mughabghab, S. F. and Garber, D. I. (1973) *Neutron Cross Sections. Volume 1. Resonance Parameters.* BNL-325, 3rd ed.
- Muramatsu, Y., Takada, Y., Matsuzaki, H. and Yoshida, S. (2008) AMS analysis of  $^{129}\text{I}$  in Japanese soil samples collected from background areas far from nuclear facilities. *Quater. Geochronol.* **3**, 291–297.
- Nichols, A. L., Aldama, D. L. and Verpelli, M. (2008) *Handbook of Nuclear Data for Safeguards: Database Extensions, August 2008*, IAEA-INDC(NDS)-0534. Available at <http://www.nds.iaea.org/publications/indc/indc-nds-0534.pdf>
- Prisyazhniuk, A., Pjatak, O., Buzanov, V. A., Reeves, G. K. and Beral, V. (1991) Cancer in the Ukraine, post-Chernobyl. *Lancet* **338**, 1334–1335.
- Sharma, P., Elmore, D., Miller, T. and Vogt, S. (1997) The  $^{129}\text{I}$  AMS program at PRIME Lab. *Nucl. Instr. Methods Phys. Res.* **B123**, 347–351.
- Shibata, K., Iwamoto, O., Nakagawa, T., Iwamoto, N., Ichihara, A., Kunieda, S., Chiba, S., Furutaka, K., Otuka, N., Ohsawa, T., Murata, T., Matsunobu, H., Zukeran, A., Kamada, S. and Katakura, J. (2011) JENDL-4.0: A new library for nuclear science and engineering. *J. Nucl. Sci. Technol.* **48**, 1–30.
- TEPCO (Tokyo Electricity Power Corporation) (2004) Available at <http://www.tepco.co.jp/cc/press/04040601-j.html> (in Japanese).
- TEPCO (2005a) Press release on the start of periodic operator inspection at Fukushima Daiichi nuclear power plant Unit 2. Available at <http://www.tepco.co.jp/cc/press/05041501-j.html> (in Japanese).
- TEPCO (2005b) Fukushima Daiichi nuclear power plant Unit 3, 20th periodic operator's inspection report. Available at <http://www.tepco.co.jp/fukushima1-np/b45306-j.pdf> (in Japanese).
- TEPCO (2005c) Fukushima Daiichi nuclear power plant Unit 2, 21st periodic operator's inspection report. Available at <http://www.tepco.co.jp/fukushima1-np/b45228-j.pdf> (in Japanese).
- TEPCO (2006) Fukushima Daiichi nuclear power plant Unit 3, 21st periodic operator's inspection report. Available at [http://www.tepco.co.jp/nu/f1-np/press\\_f1/2006/pdfdata/bi6b20-j.pdf](http://www.tepco.co.jp/nu/f1-np/press_f1/2006/pdfdata/bi6b20-j.pdf) (in Japanese).

- TEPCO (2007) Fukushima Daiichi nuclear power plant Unit 2, 22nd periodic operator's inspection report. Available at [http://www.tepco.co.jp/nu/f1-np/press\\_f1/2007/pdfdata/bi7614-j.pdf](http://www.tepco.co.jp/nu/f1-np/press_f1/2007/pdfdata/bi7614-j.pdf) (in Japanese).
- TEPCO (2008a) Fukushima Daiichi nuclear power plant Unit 1, 24th periodic operator's inspection report. Available at [http://www.tepco.co.jp/nu/f1-np/press\\_f1/2007/pdfdata/bi8116-j.pdf](http://www.tepco.co.jp/nu/f1-np/press_f1/2007/pdfdata/bi8116-j.pdf) (in Japanese).
- TEPCO (2008b) Fukushima Daiichi nuclear power plant Unit 3, 22nd periodic operator's inspection report. Available at [http://www.tepco.co.jp/nu/f1-np/press\\_f1/2007/pdfdata/bi8326-j.pdf](http://www.tepco.co.jp/nu/f1-np/press_f1/2007/pdfdata/bi8326-j.pdf) (in Japanese).
- TEPCO (2008c) Fukushima Daiichi nuclear power plant Unit 2, 23rd periodic operator's inspection report. Available at [http://www.tepco.co.jp/nu/f1-np/press\\_f1/2008/pdfdata/bi8806-j.pdf](http://www.tepco.co.jp/nu/f1-np/press_f1/2008/pdfdata/bi8806-j.pdf) (in Japanese).
- TEPCO (2009a) Fukushima Daiichi nuclear power plant Unit 2, 24th periodic operator's inspection report. Available at [http://www.tepco.co.jp/nu/f1-np/press\\_f1/2009/pdfdata/bi9a04-j.pdf](http://www.tepco.co.jp/nu/f1-np/press_f1/2009/pdfdata/bi9a04-j.pdf) (in Japanese).
- TEPCO (2009b) Fukushima Daiichi nuclear power plant Unit 3, 23rd periodic operator's inspection report. Available at [http://www.tepco.co.jp/nu/f1-np/press\\_f1/2009/pdfdata/bi9a09-j.pdf](http://www.tepco.co.jp/nu/f1-np/press_f1/2009/pdfdata/bi9a09-j.pdf) (in Japanese).
- TEPCO (2010a) Fukushima Daiichi nuclear power plant Unit 1, 26th periodic operator's inspection report. Available at [http://www.tepco.co.jp/nu/f1-np/press\\_f1/2010/pdfdata/bi0c06-j.pdf](http://www.tepco.co.jp/nu/f1-np/press_f1/2010/pdfdata/bi0c06-j.pdf) (in Japanese).
- TEPCO (2010b) Fukushima Daiichi nuclear power plant Unit 3, 24th periodic operator's inspection report. Available at [http://www.tepco.co.jp/nu/f1-np/press\\_f1/2010/pdfdata/bi0c11-j.pdf](http://www.tepco.co.jp/nu/f1-np/press_f1/2010/pdfdata/bi0c11-j.pdf) (in Japanese).
- TEPCO (2011a) The air dose rate recorded at monitoring posts of the Fukushima Daiichi NPP. Available at [http://www.tepco.co.jp/cc/press/betu11\\_j/images/110528d.pdf](http://www.tepco.co.jp/cc/press/betu11_j/images/110528d.pdf) (in Japanese).
- TEPCO (2011b) Fukushima Daiichi nuclear power plant Unit 2, 25th periodic operator's inspection report. Available at [http://www.tepco.co.jp/nu/f1-np/press\\_f1/2010/pdfdata/bi1207-j.pdf](http://www.tepco.co.jp/nu/f1-np/press_f1/2010/pdfdata/bi1207-j.pdf) (in Japanese).
- TEPCO (2011c) Overview of facility of Fukushima Daiichi Nuclear Power Station. Available at [http://www.tepco.co.jp/en/nu/fukushima-np/outline\\_f1/index-e.html](http://www.tepco.co.jp/en/nu/fukushima-np/outline_f1/index-e.html) (in Japanese).